Jet production and α_S measurements at CMS

Georgios Mavromanolakis[a] on behalf of the CMS Collaboration

[a] *University of Cyprus, Department of Physics, Nicosia, Cyprus*

Abstract

Recent CMS results related to jet production measurements as well as measurements of the strong coupling constant are discussed. In particular, results are described related to jet production cross sections, which pose a central test to perturbative QCD predictions, as well as hadronic event shape measurements, and measurements of α_S with data taken at center-of-mass energy of 7 TeV and 8 TeV collected with the CMS detector.

Keywords: *jet production cross sections, parton distribution functions, strong coupling constant*

1. Introduction

Measurements at the LHC experiments are of great importance for several reasons since they provide precise measurements of perturbative Quantum Chromodynamics (QCD) in a new energy regime, constraints on proton density functions (PDFs), measures of the strong coupling constant, studies of initial and final state radiation and parton showering effects. They also provide a precise measurement of the main background for most of the new physics searches.

2. Jet reconstruction and calibration

Jets are reconstructed using the anti-kT clustering algorithm [1] with a radius parameter R of 0.5 and 0.7. The inputs to the jet-clustering algorithm are the four-momentum vectors of reconstructed particles with the particle-flow technique [2] which combines information from several sub-detector systems. The resulting jets require an additional energy correction [3-4] to take into account the non-linear and non-uniform response of the CMS calorimetric system to the neutral-hadron component of the jet (the momentum of charged hadrons and photons is measured accurately by the tracker and the electromagnetic calorimeter, respectively). The resulting systematic uncertainty of the order of $< 1\%$ for jets with $pT > 100$ GeV.

3. Inclusive jet and dijet cross sections

Measurements of the inclusive jet and dijet cross sections can be used to test the predictions of perturbative QCD, constrain PDFs of the proton, differentiate among PDF sets, and look for possible deviations from the standard model (SM). The CMS experiment has performed measurements of the inclusive jet and dijet differential cross section with both the 7 TeV and the 8 TeV

data samples [5-8].

As shown in Fig. 1 and Fig. 2 the measured inclusive jet and dijet cross sections at 8 TeV agree nicely with perturbative QCD (pQCD) at Next-to-Leading Order (NLO) theoretical predictions over many orders of magnitude
and for all different rapidity bins considered.

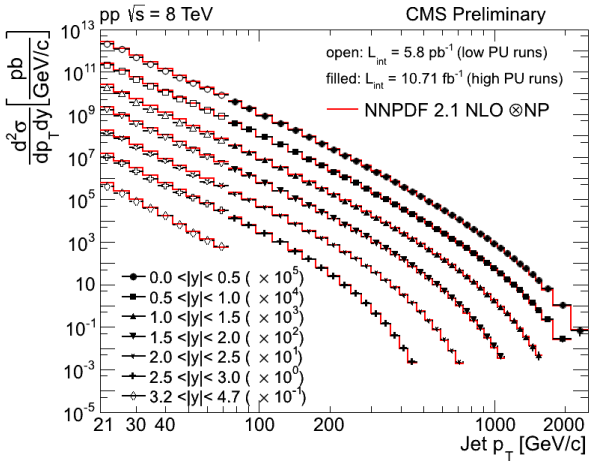

Fig. 1. The combined differential inclusive jet cross sections compared to NLO predictions using the NNPDF2.1 PDF set times the non-perturbative (NP) correction factor. Open symbols represent the measurement at 8 T using minimum bias data with low pile-up conditions and corresponding to an integrated luminosity of 5.8 pb^{-1}. Filled symbols represent the measurement utilizing higher p_T jets corresponding to an integrated luminosity of 10.71 fb^{-1}.

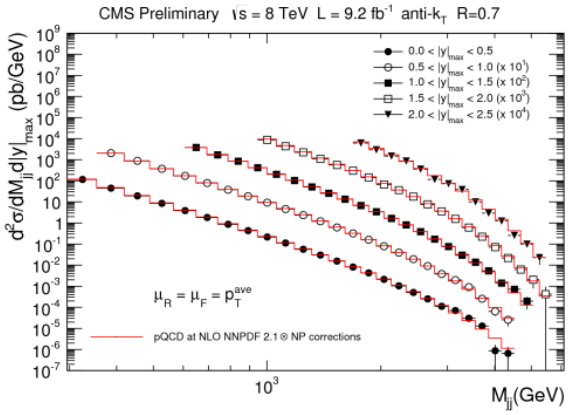

Fig. 2. The differential dijet cross sections compared to NLO predictions using the NNPDF2.1 PDF set times the non-perturbative (NP) correction factor. Markers represent the measurement at 8 TeV.

The ratio of the measured jet cross sections to the theoretical predictions using different PDF sets is shown in Fig. 3 and Fig. 4. There is good agreement between the two, and given that the experimental and theoretical uncertainties are comparable, these measurements have already been used to constraint gluon PDFs.

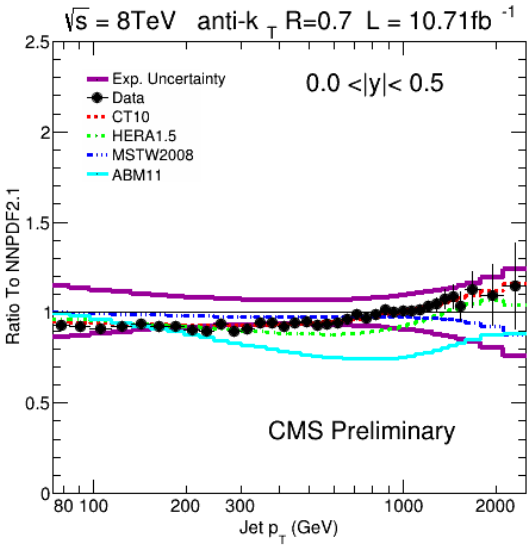

Fig. 3 The data (inclusive jet cross section) over theory distribution for NNPDF2.1 PDF set is compared with the ratio of other PDF sets to NNPDF2.1 for the central rapidity bin. The total experimental uncertainty band is shown in magenta. The data over theory distribution are shown by black dots.

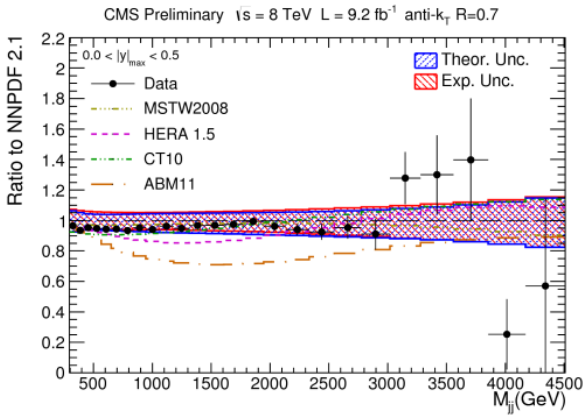

Fig. 4 The data (dijet cross section) over theory distribution for NNPDF2.1 PDF set is compared with the ratio of other PDF sets to NNPDF2.1 for the central rapidity bin. The total experimental uncertainty band is shown in red and the total theoretical one in blue. The data over theory distribution are shown by black dots.

4. Hadronic Event Shapes

Event-shape variables measure the properties of the energy flow in the final states of high-energy particle collisions. They are sensitive to perturbative and

nonperturbative aspects of QCD interactions. At CMS they are studied in multijet events recorded in proton-proton collisions at a centre-of-mass energy of 7 TeV [9]. The event shape variables that have been studied are thea) **Transverse Thrust,** which is sensitive to the modeling of two-jet and multijet topologies. For a perfectly balanced two-jet event it is zero, while in isotropic multi-jet events it is (1-2/π). b) **Jet Broadenings,** which are insensitive to the contribution of the underlying event and hadronization and sensitive to color coherence effects. c) **Jet Masses,** which show the same behavior and dependence as jet broadenings but are more sensitive to (initial state) forward radiation, and d) **Jet Resolution**, which estimates the relative strength of the p_T of the third jet with respect to the other two jets. It is zero for two-jet events, a non-zero value indicates the presence of hard parton emission and it is sensitive to the parton showering modeling.

For the transverse thrust and the total transverse jet mass, all generators show an overall 10% - 20% agreement with the data respectively. However, as shown in Fig. 5, event-shape variables that are more sensitive to the longitudinal energy flow (such as the total jet mass), or to hard parton emissions (such as the jet broadening) show a larger discrepancy between data and parton shower MC simulations. The modeling of colour connection between the soft scatters and beam remnants, and initial- and final-state radiations are the major sources of differences between the various QCD event generators.

5. Multijet Events

Kinematic and angular distributions in inclusive multijet final states serve as a natural probe of quantum chromodynamics and can reveal its inner dynamics [10].

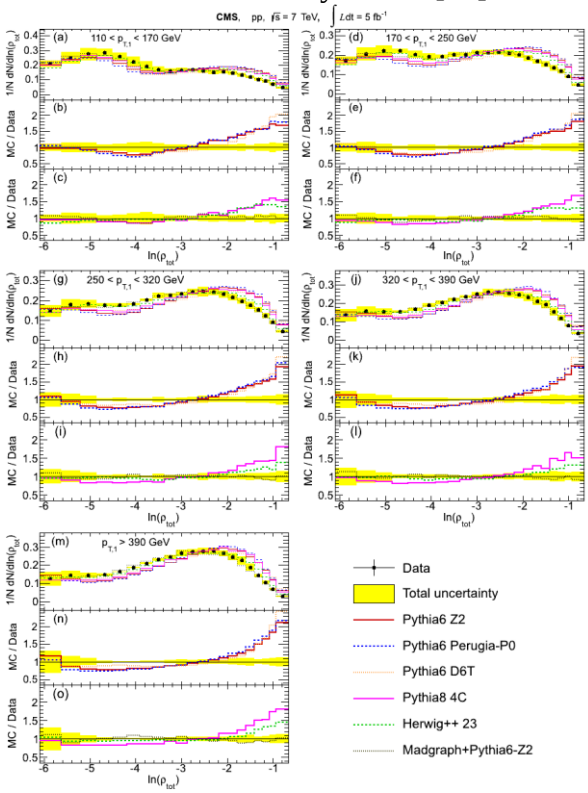

Fig. 5(a,d,g,j,m) Comparison between the total jet mass distributions in data and various event generators in five different ranges of transverse momentum. The error bars indicate the statistical uncertainties and the shaded yellow bands represent the statistical and systematic uncertainties suqred. The panels (b,e,h,k,n) show the ratios of different models of PYTHIA6 event generator over data in each momentum range and panels (c,f,i,l,o) show the ratios for other generators.

Their study helps to validate and tune theoretical models implemented in various QCD event generators. Studies of three-jet events involve three-jet mass and the scaled energy distributions of the jets in the three-jet centre of mass system. For four jet events, results are presented for four-jet mass and two event plane angles: One is the Bengtsson-Zerwas angle (BZ) [11] defined as the angle between the plane containing the two leading jets and the plane containing the two non-leading jets.

The second variable is the cosine of the Nachtmann-Reiter angle (NR) [12] defined as the angle between the momentum vector differences of the two leading jets and the

two non-leading jets. Comparisons are carried out with the data and predictions of leading order calculations and parton shower generators. Figures 6 and 7 show the distribution of scaled energy of the second leading jet being compared with predictions from four different Monte Carlo models

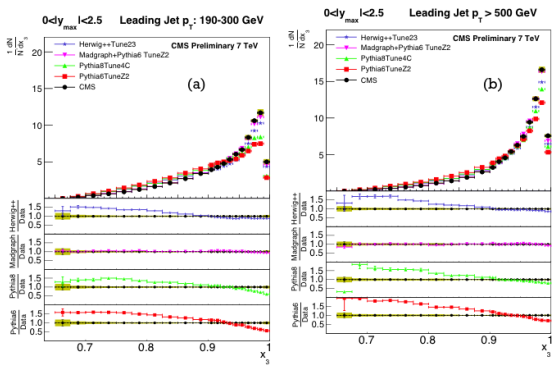

Fig. 6 Distribution of scaled energy of the leading jet being compared with predictions from four Monte Carlo models: Pythia6, Pythia8, Madgraph+Pythia6, Herwig++. The distributions are obtained from inclusive three-jet sample with the jets restricted in the y-region 0.0:2.5 and with leading jet p_T between (a) 190 and 300 GeV or (b) above 500 GeV. The data points are shown with statistical uncertainty only and the bands indicate the statistical and systematic uncertainties combined in quadrature. The bottom part of each plot shows the ratio of Monte Carlo predictions to the data. The ratios are shown with statistical uncertainty in the data as well as in the Monte Carlo while the band shows combined statistical and systematic uncertainties.

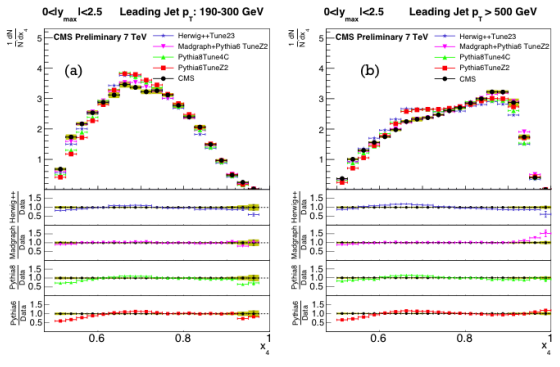

Fig. 7 Distribution of scaled energy of the second leading jet being compared with predictions from four Monte Carlo models: Pythia6, Pythia8, Madgraph+Pythia6, Herwig++. The distributions are obtained from inclusive three-jet sample with the jets restricted in the y-region 0.0:2.5 and with leading jet p_T between (a) 190 and 300 GeV or (b) above 500 GeV The data points are shown with statistical uncertainty only and the bands indicate the statistical and systematic uncertainties combined in quadrature. The bottom part of each plot shows the ratio of Monte Carlo predictions to the data. The ratios are shown with statistical uncertainty in the data as well as in the Monte Carlo while the band shows combined statistical and systematic uncertainties.

In general, all Monte Carlo models with only leading order calculations for dijet production cannot provide a satisfactory description of all multijet distributions. The compared data results are corrected for detector effects in order to be can be directly compared with other models or next-to-leading order theoretical predictions.

6. Measurements of the strong coupling constant

The measurements of the strong coupling constant (α_S) are of great importance not only because they are probing the most fundamental QCD quantity, but also because its running, especially at high momentum transfer (Q), is sensitive to new physics like Supersymmetry [13] and extra spacetime dimensions [14]. The CMS experiment has recently reported on three different measurements of the strong coupling constant using jets in the final state. The first one uses the ratio of events with three and two jets [15] in the final state. The advantage of this measurement is that most of the experimental as well as theoretical uncertainties are canceled, while on the same time this ratio is sensitive to the value of the strong coupling constant as shown in Fig.8.

The second one uses the measurement of the double-differential 3-jet mass cross section [16]. This observable at LO is proportional to α_S^3, and theory predictions are available up to NLO order such that precise comparisons to data are possible. In Figure 9 the ratio of the unfolded 3-jet mass distribution to the theory prediction including NP effects using PDF sets with NNLO PDF evolution in the inner rapidity bin is shown.

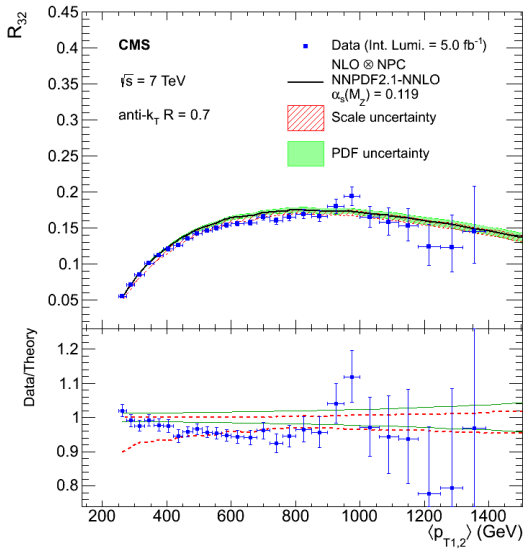

Fig. 8 Measurement of R_{32} and NLO predictions using the NNPDF2.1 NNLO PDF sets. In the upper panel, the ratio R_{32} (solid circles) together with the NLO prediction (black line), the scale uncertainty (red band) and the PDF uncertainty (green band) are shown. The bottom panel shows the ratio of data to the theoretical predictions, together with bands representing the scale (red dotted lines) and PDF (green solid lines) uncertainties. The error bars correspond to the total uncertainty. For each PDF set the respective default value of $\alpha_S(M_Z)$ is used as indicated

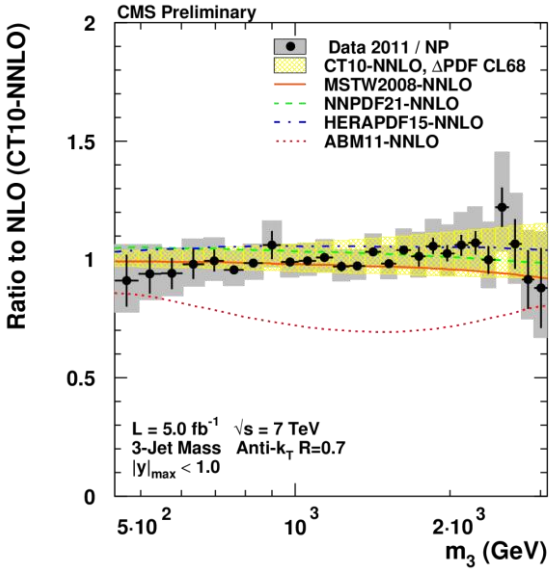

Fig. 9 Ratio of the unfolded 3-jet mass distribution to the theory prediction including NP effects using PDF sets with NNLO PDF evolution in the inner rapidity bin. The data are shown with error bars representing the statistical uncertainty and gray squares for the systematic uncertainties. The PDF uncertainty is shown for the CT10 PDF set at 68% confidence level as yellow band. In addition the central predictions are displayed for the other four examined PDF sets MSTW2008, NNPDF2.1, HERAPDF1.5, and ABM11.

The third measurement used as an independent and complementary way for the extraction of the strong coupling constant is the differential inclusive jet cross section as presented previously [5].

The running of strong coupling constant is shown in Fig. 10 with the CMS measurements populating the very interesting high Q values, and being the first ones to have exceeding the 1 TeV scale.

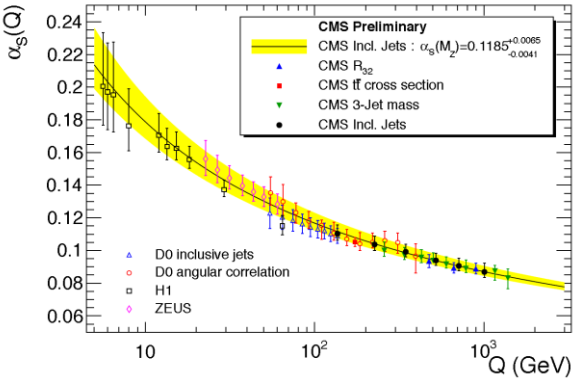

Fig. 10 Comparison of the evolution of the strong coupling constant from all CMS measurements to the world average (upper curve). The error bars on the data points correspond to the total uncertainty. In addition an overview of measurements of the running of the strong coupling constant from electron-positron collider experiments, electron-proton experiments, and proton/anti-proton collider experiments is presented. The results of the CMS analysis extend the covered range to high scales Q up to ~ 1.4 TeV.

In addition, the CMS measurements of this fundamental quantity are one of the most precise ever made as shown in Fig. 11

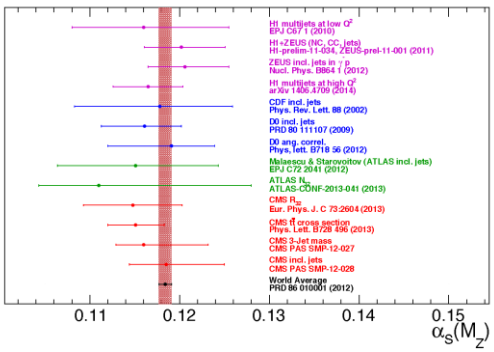

Fig. 11 Measurements of the strong coupling constant from various experiments.

7. Summary

A selection of recent jet measurements from

the CMS collaboration has been discussed. These measurements are important for a variety of studies: from constraining and tunning PDFs to better understanding of different MC models and the extraction of the strong coupling constant and its running.

References

[1] M. Cacciari, G. P. Salam, and G. Soyez, "The anti-kT jet clustering algorithm", JHEP 04 295 (2008) 063, doi:10.1088/1126-6708/2008/04/063.

[2] CMS Collaboration, "Particle-flow Event Reconstruction in CMS and Performance for Jets, Taus, and MET",CMS Physics Analysis Summary CMS-PAS-PFT-09-001, (2009).

[3] CMS Collaboration, "Determination of jet energy calibration and transverse momentum resolution in CMS" J. Instrum. 6 (2011) P11002, 300 doi:10.1088/1748-0221/6/11/P11002.

[4] CMS collaboration, "Status of the 8 TeV Jet Energy Corrections and Uncertainties based on 19.8 fb^{-1} of data in CMS", CMS DP-2013/033

[5] CMS Collaboration, "Measurements of differential jet cross sections in proton-proton collisions at sqrt{s}= 7 TeV with the CMS detector", Phys. Rev. D 87 (2013) 112002

[6] CMS Collaboration, "Measurement of the double-differential inclusive jet cross section at sqrt(s) = 8 TeV with the CMS detector ", CMS Physics Analysis Summary CMS-PAS-SMP-12-012 (2012)

[7] CMS Collaboration, "Measurement of jet cross sections at low transverse momentum in proton-proton collisions at 8 TeV", CMS Physics Analysis Summary CMS-PAS-FSQ-12-031 (2012)

[8] CMS Collaboration, "Measurements of differential dijet cross section in proton-proton collisions at sqrt(s)=8 TeV with the CMS detector", CMS Physics Analysis Summary CMS-PAS-SMP-14-02 (2014)

[9] CMS Collaboration, "Study of hadronic event-shape variables in multijet final states in pp collisions at sqrt{s} = 7 TeV", CMS Physics Analysis Summary CMS-PAS-SMP-12-022 (2013), arXiv:1407.2856, submitted to JHEP.

[10] CMS Collaboration, "Study of Topological Distributions of Inclusive Three and Four-jet Events at the LHC", CMS Physics Analysis Summary CMS-PAS-QCD-11-006.

[11] M. Bengtsson and P. M. Zerwas, "Four-jet events in e^+e^- annihilation: Testing the three-gluon vertex", Phys. Lett. B 208 (1988) 306, doi:10.1016/0370-2693(88)90435-2.

[12] O. Nachtmann and A. Reiter, "A test for the gluon selfcoupling in the reactions e+e→4 jets and Z→4 jets", Z. Phys. C 16 (1982) 45, doi:10.1007/BF01573746.

[13] Chris Quigg, "Beyond Confinement", arXiv:1301.4905 [hep-ph]

[14] K.Dienes , E.Dudas, T. Gherghetta , "Grand unifcation at intermediate mass scales through extra dimensions", Nucl.Phys. B537 (1999) 47-108

[15] CMS Collaboration, "Measurement of the ratio of the inclusive 3-jet cross section to the inclusive 2-jet cross section in pp collisions at sqrt{s} = 7 TeV and first determination of the strong coupling constant in the TeV range", Eur.Phys.J. C73 (2013)2604.